Improved Limits on the Lepton-Flavor Violating Decays $\tau^- \to l^- l^+ l^-$

B. Aubert,[1] M. Bona,[1] D. Boutigny,[1] Y. Karyotakis,[1] J. P. Lees,[1] V. Poireau,[1] X. Prudent,[1] V. Tisserand,[1] A. Zghiche,[1]
J. Garra Tico,[2] E. Grauges,[2] L. Lopez,[3] A. Palano,[3] M. Pappagallo,[3] G. Eigen,[4] B. Stugu,[4] L. Sun,[4] G. S. Abrams,[5]
M. Battaglia,[5] D. N. Brown,[5] J. Button-Shafer,[5] R. N. Cahn,[5] Y. Groysman,[5] R. G. Jacobsen,[5] J. A. Kadyk,[5] L. T. Kerth,[5]
Yu. G. Kolomensky,[5] G. Kukartsev,[5] D. Lopes Pegna,[5] G. Lynch,[5] L. M. Mir,[5] T. J. Orimoto,[5] I. L. Osipenkov,[5]
M. T. Ronan,[5,*] K. Tackmann,[5] T. Tanabe,[5] W. A. Wenzel,[5] P. del Amo Sanchez,[6] C. M. Hawkes,[6] A. T. Watson,[6] H. Koch,[7]
T. Schroeder,[7] D. Walker,[8] D. J. Asgeirsson,[9] T. Cuhadar-Donszelmann,[9] B. G. Fulsom,[9] C. Hearty,[9] T. S. Mattison,[9]
J. A. McKenna,[9] M. Barrett,[10] A. Khan,[10] M. Saleem,[10] L. Teodorescu,[10] V. E. Blinov,[11] A. D. Bukin,[11] V. P. Druzhinin,[11]
V. B. Golubev,[11] A. P. Onuchin,[11] S. I. Serednyakov,[11] Yu. I. Skovpen,[11] E. P. Solodov,[11] K. Yu. Todyshev,[11] M. Bondioli,[12]
S. Curry,[12] I. Eschrich,[12] D. Kirkby,[12] A. J. Lankford,[12] P. Lund,[12] M. Mandelkern,[12] E. C. Martin,[12] D. P. Stoker,[12]
S. Abachi,[13] C. Buchanan,[13] S. D. Foulkes,[14] J. W. Gary,[14] F. Liu,[14] O. Long,[14] B. C. Shen,[14] G. M. Vitug,[14] L. Zhang,[14]
H. P. Paar,[15] S. Rahatlou,[15] V. Sharma,[15] J. W. Berryhill,[16] C. Campagnari,[16] A. Cunha,[16] B. Dahmes,[16] T. M. Hong,[16]
D. Kovalskyi,[16] J. D. Richman,[16] T. W. Beck,[17] A. M. Eisner,[17] C. J. Flacco,[17] C. A. Heusch,[17] J. Kroseberg,[17]
W. S. Lockman,[17] T. Schalk,[17] B. A. Schumm,[17] A. Seiden,[17] M. G. Wilson,[17] L. O. Winstrom,[17] E. Chen,[18] C. H. Cheng,[18]
F. Fang,[18] D. G. Hitlin,[18] I. Narsky,[18] T. Piatenko,[18] F. C. Porter,[18] R. Andreassen,[19] G. Mancinelli,[19] B. T. Meadows,[19]
K. Mishra,[19] M. D. Sokoloff,[19] F. Blanc,[20] P. C. Bloom,[20] S. Chen,[20] W. T. Ford,[20] J. F. Hirschauer,[20] A. Kreisel,[20]
M. Nagel,[20] U. Nauenberg,[20] A. Olivas,[20] J. G. Smith,[20] K. A. Ulmer,[20] S. R. Wagner,[20] J. Zhang,[20] A. M. Gabareen,[21]
A. Soffer,[21,†] W. H. Toki,[21] R. J. Wilson,[21] F. Winklmeier,[21] D. D. Altenburg,[22] E. Feltresi,[22] A. Hauke,[22] H. Jasper,[22]
J. Merkel,[22] A. Petzold,[22] B. Spaan,[22] K. Wacker,[22] V. Klose,[23] M. J. Kobel,[23] H. M. Lacker,[23] W. F. Mader,[23]
R. Nogowski,[23] J. Schubert,[23] K. R. Schubert,[23] R. Schwierz,[23] J. E. Sundermann,[23] A. Volk,[23] D. Bernard,[24]
G. R. Bonneaud,[24] E. Latour,[24] V. Lombardo,[24] Ch. Thiebaux,[24] M. Verderi,[24] P. J. Clark,[25] W. Gradl,[25] F. Muheim,[25]
S. Playfer,[25] A. I. Robertson,[25] J. E. Watson,[25] Y. Xie,[25] M. Andreotti,[26] D. Bettoni,[26] C. Bozzi,[26] R. Calabrese,[26]
A. Cecchi,[26] G. Cibinetto,[26] P. Franchini,[26] E. Luppi,[26] M. Negrini,[26] A. Petrella,[26] L. Piemontese,[26] E. Prencipe,[26]
V. Santoro,[26] F. Anulli,[27] R. Baldini-Ferroli,[27] A. Calcaterra,[27] R. de Sangro,[27] G. Finocchiaro,[27] S. Pacetti,[27] P. Patteri,[27]
I. M. Peruzzi,[27,‡] M. Piccolo,[27] M. Rama,[27] A. Zallo,[27] A. Buzzo,[28] R. Contri,[28] M. Lo Vetere,[28] M. M. Macri,[28]
M. R. Monge,[28] S. Passaggio,[28] C. Patrignani,[28] E. Robutti,[28] A. Santroni,[28] S. Tosi,[28] K. S. Chaisanguanthum,[29]
M. Morii,[29] J. Wu,[29] R. S. Dubitzky,[30] J. Marks,[30] S. Schenk,[30] U. Uwer,[30] D. J. Bard,[31] P. D. Dauncey,[31] R. L. Flack,[31]
J. A. Nash,[31] W. Panduro Vazquez,[31] M. Tibbetts,[31] P. K. Behera,[32] X. Chai,[32] M. J. Charles,[32] U. Mallik,[32] J. Cochran,[33]
H. B. Crawley,[33] L. Dong,[33] V. Eyges,[33] W. T. Meyer,[33] S. Prell,[33] E. I. Rosenberg,[33] A. E. Rubin,[33] Y. Y. Gao,[34]
A. V. Gritsan,[34] Z. J. Guo,[34] C. K. Lae,[34] A. G. Denig,[35] M. Fritsch,[35] G. Schott,[35] N. Arnaud,[36] J. Béquilleux,[36]
A. D'Orazio,[36] M. Davier,[36] G. Grosdidier,[36] A. Höcker,[36] V. Lepeltier,[36] F. Le Diberder,[36] A. M. Lutz,[36] S. Pruvot,[36]
S. Rodier,[36] P. Roudeau,[36] M. H. Schune,[36] J. Serrano,[36] V. Sordini,[36] A. Stocchi,[36] W. F. Wang,[36] G. Wormser,[36]
D. J. Lange,[37] D. M. Wright,[37] I. Bingham,[38] J. P. Burke,[38] C. A. Chavez,[38] J. R. Fry,[38] E. Gabathuler,[38] R. Gamet,[38]
D. E. Hutchcroft,[38] D. J. Payne,[38] K. C. Schofield,[38] C. Touramanis,[38] A. J. Bevan,[39] K. A. George,[39] F. Di Lodovico,[39]
R. Sacco,[39] G. Cowan,[40] H. U. Flaecher,[40] D. A. Hopkins,[40] S. Paramesvaran,[40] F. Salvatore,[40] A. C. Wren,[40]
D. N. Brown,[41] C. L. Davis,[41] J. Allison,[42] D. Bailey,[42] N. R. Barlow,[42] R. J. Barlow,[42] Y. M. Chia,[42] C. L. Edgar,[42]
G. D. Lafferty,[42] T. J. West,[42] J. I. Yi,[42] J. Anderson,[43] C. Chen,[43] A. Jawahery,[43] D. A. Roberts,[43] G. Simi,[43] J. M. Tuggle,[43]
G. Blaylock,[44] C. Dallapiccola,[44] S. S. Hertzbach,[44] X. Li,[44] T. B. Moore,[44] E. Salvati,[44] S. Saremi,[44] R. Cowan,[45]
D. Dujmic,[45] P. H. Fisher,[45] K. Koeneke,[45] G. Sciolla,[45] M. Spitznagel,[45] F. Taylor,[45] R. K. Yamamoto,[45] M. Zhao,[45]
Y. Zheng,[45] S. E. Mclachlin,[46,*] P. M. Patel,[46] S. H. Robertson,[46] A. Lazzaro,[47] F. Palombo,[47] J. M. Bauer,[48] L. Cremaldi,[48]
V. Eschenburg,[48] R. Godang,[48] R. Kroeger,[48] D. A. Sanders,[48] D. J. Summers,[48] H. W. Zhao,[48] S. Brunet,[49] D. Côté,[49]
M. Simard,[49] P. Taras,[49] F. B. Viaud,[49] H. Nicholson,[50] G. De Nardo,[51] F. Fabozzi,[51,§] L. Lista,[51] D. Monorchio,[51]
C. Sciacca,[51] M. A. Baak,[52] G. Raven,[52] H. L. Snoek,[52] C. P. Jessop,[53] K. J. Knoepfel,[53] J. M. LoSecco,[53] G. Benelli,[54]
L. A. Corwin,[54] K. Honscheid,[54] H. Kagan,[54] R. Kass,[54] J. P. Morris,[54] A. M. Rahimi,[54] J. J. Regensburger,[54] S. J. Sekula,[54]
Q. K. Wong,[54] N. L. Blount,[55] J. Brau,[55] R. Frey,[55] O. Igonkina,[55] J. A. Kolb,[55] M. Lu,[55] R. Rahmat,[55] N. B. Sinev,[55]
D. Strom,[55] J. Strube,[55] E. Torrence,[55] N. Gagliardi,[56] A. Gaz,[56] M. Margoni,[56] M. Morandin,[56] A. Pompili,[56]
M. Posocco,[56] M. Rotondo,[56] F. Simonetto,[56] R. Stroili,[56] C. Voci,[56] E. Ben-Haim,[57] H. Briand,[57] G. Calderini,[57]
J. Chauveau,[57] P. David,[57] L. Del Buono,[57] Ch. de la Vaissière,[57] O. Hamon,[57] Ph. Leruste,[57] J. Malclès,[57] J. Ocariz,[57]
A. Perez,[57] J. Prendki,[57] L. Gladney,[58] M. Biasini,[59] R. Covarelli,[59] E. Manoni,[59] C. Angelini,[60] G. Batignani,[60]

S. Bettarini,[60] M. Carpinelli,[60] R. Cenci,[60] A. Cervelli,[60] F. Forti,[60] M. A. Giorgi,[60] A. Lusiani,[60] G. Marchiori,[60] M. A. Mazur,[60] M. Morganti,[60] N. Neri,[60] E. Paoloni,[60] G. Rizzo,[60] J. J. Walsh,[60] J. Biesiada,[61] P. Elmer,[61] Y. P. Lau,[61] C. Lu,[61] J. Olsen,[61] A. J. S. Smith,[61] A. V. Telnov,[61] E. Baracchini,[62] F. Bellini,[62] G. Cavoto,[62] D. del Re,[62] E. Di Marco,[62] R. Faccini,[62] F. Ferrarotto,[62] F. Ferroni,[62] M. Gaspero,[62] P. D. Jackson,[62] L. Li Gioi,[62] M. A. Mazzoni,[62] S. Morganti,[62] G. Piredda,[62] F. Polci,[62] F. Renga,[62] C. Voena,[62] M. Ebert,[63] T. Hartmann,[63] H. Schröder,[63] R. Waldi,[63] T. Adye,[64] G. Castelli,[64] B. Franek,[64] E. O. Olaiya,[64] W. Roethel,[64] F. F. Wilson,[64] S. Emery,[65] M. Escalier,[65] A. Gaidot,[65] S. F. Ganzhur,[65] G. Hamel de Monchenault,[65] W. Kozanecki,[65] G. Vasseur,[65] Ch. Yèche,[65] M. Zito,[65] X. R. Chen,[66] H. Liu,[66] W. Park,[66] M. V. Purohit,[66] R. M. White,[66] J. R. Wilson,[66] M. T. Allen,[67] D. Aston,[67] R. Bartoldus,[67] P. Bechtle,[67] R. Claus,[67] J. P. Coleman,[67] M. R. Convery,[67] J. C. Dingfelder,[67] J. Dorfan,[67] G. P. Dubois-Felsmann,[67] W. Dunwoodie,[67] R. C. Field,[67] T. Glanzman,[67] S. J. Gowdy,[67] M. T. Graham,[67] P. Grenier,[67] C. Hast,[67] W. R. Innes,[67] J. Kaminski,[67] M. H. Kelsey,[67] H. Kim,[67] P. Kim,[67] M. L. Kocian,[67] D. W. G. S. Leith,[67] S. Li,[67] S. Luitz,[67] V. Luth,[67] H. L. Lynch,[67] D. B. MacFarlane,[67] H. Marsiske,[67] R. Messner,[67] D. R. Muller,[67] C. P. O'Grady,[67] I. Ofte,[67] A. Perazzo,[67] M. Perl,[67] T. Pulliam,[67] B. N. Ratcliff,[67] A. Roodman,[67] A. A. Salnikov,[67] R. H. Schindler,[67] J. Schwiening,[67] A. Snyder,[67] D. Su,[67] M. K. Sullivan,[67] K. Suzuki,[67] S. K. Swain,[67] J. M. Thompson,[67] J. Va'vra,[67] A. P. Wagner,[67] M. Weaver,[67] W. J. Wisniewski,[67] M. Wittgen,[67] D. H. Wright,[67] A. K. Yarritu,[67] K. Yi,[67] C. C. Young,[67] V. Ziegler,[67] P. R. Burchat,[68] A. J. Edwards,[68] S. A. Majewski,[68] T. S. Miyashita,[68] B. A. Petersen,[68] L. Wilden,[68] S. Ahmed,[69] M. S. Alam,[69] R. Bula,[69] J. A. Ernst,[69] V. Jain,[69] B. Pan,[69] M. A. Saeed,[69] F. R. Wappler,[69] S. B. Zain,[69] M. Krishnamurthy,[70] S. M. Spanier,[70] R. Eckmann,[71] J. L. Ritchie,[71] A. M. Ruland,[71] C. J. Schilling,[71] R. F. Schwitters,[71] J. M. Izen,[72] X. C. Lou,[72] S. Ye,[72] F. Bianchi,[73] F. Gallo,[73] D. Gamba,[73] M. Pelliccioni,[73] M. Bomben,[74] L. Bosisio,[74] C. Cartaro,[74] F. Cossutti,[74] G. Della Ricca,[74] L. Lanceri,[74] L. Vitale,[74] V. Azzolini,[75] N. Lopez-March,[75] F. Martinez-Vidal,[75,||] D. A. Milanes,[75] A. Oyanguren,[75] J. Albert,[76] Sw. Banerjee,[76] B. Bhuyan,[76] K. Hamano,[76] R. Kowalewski,[76] I. M. Nugent,[76] J. M. Roney,[76] R. J. Sobie,[76] P. F. Harrison,[77] J. Ilic,[77] T. E. Latham,[77] G. B. Mohanty,[77] H. R. Band,[78] X. Chen,[78] S. Dasu,[78] K. T. Flood,[78] J. J. Hollar,[78] P. E. Kutter,[78] Y. Pan,[78] M. Pierini,[78] R. Prepost,[78] S. L. Wu,[78] and H. Neal[79]

(*BABAR* Collaboration)

[1]*Laboratoire de Physique des Particules, IN2P3/CNRS et Université de Savoie, F-74941 Annecy-Le-Vieux, France*
[2]*Universitat de Barcelona, Facultat de Fisica, Departament ECM, E-08028 Barcelona, Spain*
[3]*Università di Bari, Dipartimento di Fisica and INFN, I-70126 Bari, Italy*
[4]*University of Bergen, Institute of Physics, N-5007 Bergen, Norway*
[5]*Lawrence Berkeley National Laboratory and University of California, Berkeley, California 94720, USA*
[6]*University of Birmingham, Birmingham, B15 2TT, United Kingdom*
[7]*Ruhr Universität Bochum, Institut für Experimentalphysik 1, D-44780 Bochum, Germany*
[8]*University of Bristol, Bristol BS8 1TL, United Kingdom*
[9]*University of British Columbia, Vancouver, British Columbia, Canada V6T 1Z1*
[10]*Brunel University, Uxbridge, Middlesex UB8 3PH, United Kingdom*
[11]*Budker Institute of Nuclear Physics, Novosibirsk 630090, Russia*
[12]*University of California at Irvine, Irvine, California 92697, USA*
[13]*University of California at Los Angeles, Los Angeles, California 90024, USA*
[14]*University of California at Riverside, Riverside, California 92521, USA*
[15]*University of California at San Diego, La Jolla, California 92093, USA*
[16]*University of California at Santa Barbara, Santa Barbara, California 93106, USA*
[17]*University of California at Santa Cruz, Institute for Particle Physics, Santa Cruz, California 95064, USA*
[18]*California Institute of Technology, Pasadena, California 91125, USA*
[19]*University of Cincinnati, Cincinnati, Ohio 45221, USA*
[20]*University of Colorado, Boulder, Colorado 80309, USA*
[21]*Colorado State University, Fort Collins, Colorado 80523, USA*
[22]*Universität Dortmund, Institut für Physik, D-44221 Dortmund, Germany*
[23]*Technische Universität Dresden, Institut für Kern- und Teilchenphysik, D-01062 Dresden, Germany*
[24]*Laboratoire Leprince-Ringuet, CNRS/IN2P3, Ecole Polytechnique, F-91128 Palaiseau, France*
[25]*University of Edinburgh, Edinburgh EH9 3JZ, United Kingdom*
[26]*Università di Ferrara, Dipartimento di Fisica and INFN, I-44100 Ferrara, Italy*
[27]*Laboratori Nazionali di Frascati dell'INFN, I-00044 Frascati, Italy*
[28]*Università di Genova, Dipartimento di Fisica and INFN, I-16146 Genova, Italy*
[29]*Harvard University, Cambridge, Massachusetts 02138, USA*
[30]*Universität Heidelberg, Physikalisches Institut, Philosophenweg 12, D-69120 Heidelberg, Germany*

[31]Imperial College London, London, SW7 2AZ, United Kingdom

[32]University of Iowa, Iowa City, Iowa 52242, USA

[33]Iowa State University, Ames, Iowa 50011-3160, USA

[34]Johns Hopkins University, Baltimore, Maryland 21218, USA

[35]Universität Karlsruhe, Institut für Experimentelle Kernphysik, D-76021 Karlsruhe, Germany

[36]Laboratoire de l'Accélérateur Linéaire, IN2P3/CNRS et Université Paris-Sud 11, Centre Scientifique d'Orsay,
B. P. 34, F-91898 ORSAY Cedex, France

[37]Lawrence Livermore National Laboratory, Livermore, California 94550, USA

[38]University of Liverpool, Liverpool L69 7ZE, United Kingdom

[39]Queen Mary, University of London, E1 4NS, United Kingdom

[40]University of London, Royal Holloway and Bedford New College, Egham, Surrey TW20 0EX, United Kingdom

[41]University of Louisville, Louisville, Kentucky 40292, USA

[42]University of Manchester, Manchester M13 9PL, United Kingdom

[43]University of Maryland, College Park, Maryland 20742, USA

[44]University of Massachusetts, Amherst, Massachusetts 01003, USA

[45]Massachusetts Institute of Technology, Laboratory for Nuclear Science, Cambridge, Massachusetts 02139, USA

[46]McGill University, Montréal, Québec, Canada H3A 2T8

[47]Università di Milano, Dipartimento di Fisica and INFN, I-20133 Milano, Italy

[48]University of Mississippi, University, Mississippi 38677, USA

[49]Université de Montréal, Physique des Particules, Montréal, Québec, Canada H3C 3J7

[50]Mount Holyoke College, South Hadley, Massachusetts 01075, USA

[51]Università di Napoli Federico II, Dipartimento di Scienze Fisiche and INFN, I-80126, Napoli, Italy

[52]NIKHEF, National Institute for Nuclear Physics and High Energy Physics, NL-1009 DB Amsterdam, The Netherlands

[53]University of Notre Dame, Notre Dame, Indiana 46556, USA

[54]Ohio State University, Columbus, Ohio 43210, USA

[55]University of Oregon, Eugene, Oregon 97403, USA

[56]Università di Padova, Dipartimento di Fisica and INFN, I-35131 Padova, Italy

[57]Laboratoire de Physique Nucléaire et de Hautes Energies, IN2P3/CNRS, Université Pierre et Marie Curie-Paris6,
Université Denis Diderot-Paris7, F-75252 Paris, France

[58]University of Pennsylvania, Philadelphia, Pennsylvania 19104, USA

[59]Università di Perugia, Dipartimento di Fisica and INFN, I-06100 Perugia, Italy

[60]Università di Pisa, Dipartimento di Fisica, Scuola Normale Superiore and INFN, I-56127 Pisa, Italy

[61]Princeton University, Princeton, New Jersey 08544, USA

[62]Università di Roma La Sapienza, Dipartimento di Fisica and INFN, I-00185 Roma, Italy

[63]Universität Rostock, D-18051 Rostock, Germany

[64]Rutherford Appleton Laboratory, Chilton, Didcot, Oxon, OX11 0QX, United Kingdom

[65]DSM/Dapnia, CEA/Saclay, F-91191 Gif-sur-Yvette, France

[66]University of South Carolina, Columbia, South Carolina 29208, USA

[67]Stanford Linear Accelerator Center, Stanford, California 94309, USA

[68]Stanford University, Stanford, California 94305-4060, USA

[69]State University of New York, Albany, New York 12222, USA

[70]University of Tennessee, Knoxville, Tennessee 37996, USA

[71]University of Texas at Austin, Austin, Texas 78712, USA

[72]University of Texas at Dallas, Richardson, Texas 75083, USA

[73]Università di Torino, Dipartimento di Fisica Sperimentale and INFN, I-10125 Torino, Italy

[74]Università di Trieste, Dipartimento di Fisica and INFN, I-34127 Trieste, Italy

[75]IFIC, Universitat de Valencia-CSIC, E-46071 Valencia, Spain

[76]University of Victoria, Victoria, British Columbia, Canada V8W 3P6

[77]Department of Physics, University of Warwick, Coventry CV4 7AL, United Kingdom

[78]University of Wisconsin, Madison, Wisconsin 53706, USA

[79]Yale University, New Haven, Connecticut 06511, USA

A search for the neutrinoless, lepton-flavor violating decay of the tau lepton into three charged leptons has been performed using 376 fb^{-1} of data collected at an e^+e^- center-of-mass energy around 10.58 GeV with the *BABAR* detector at the SLAC PEP-II storage rings. In all six decay modes considered, the numbers of events found in data are compatible with the background expectations. Upper limits on the branching fractions are set in the range $(4$–$8) \times 10^{-8}$ at 90% confidence level.

Lepton-flavor violation (LFV) involving charged leptons has never been observed, and stringent experimental limits exist from muon branching fractions: $\mathcal{B}(\mu \to e\gamma) <$ 1.2×10^{-11} [1] and $\mathcal{B}(\mu \to eee) < 1.0 \times 10^{-12}$ [2] at 90% confidence level (C.L.). Recent results from neutrino oscillation experiments [3] show that LFV does indeed occur, although the branching fractions expected in charged lepton decays due to neutrino mixing alone are probably no more than 10^{-14} [4].

In tau decays, the most stringent limit on LFV is $\mathcal{B}(\tau \to \mu\gamma) < 4.5 \times 10^{-8}$ at 90% C.L. [5]. Many descriptions of physics beyond the standard model (SM), particularly models seeking to describe neutrino mixing, predict enhanced LFV in tau decays over muon decays with branching fractions from 10^{-10} up to the current experimental limits [6–8]. An observation of LFV in tau decays would be a clear signature of non-SM physics, while improved limits will provide further constraints on theoretical models.

This Letter presents a search for LFV in the neutrinoless decay $\tau^- \to \ell^-\ell^+\ell^-$, where ℓ is an electron or muon. All possible lepton combinations consistent with charge conservation are considered, leading to six distinct decay modes $(e^-e^+e^-, \mu^+e^-e^-, \mu^-e^+e^-, e^+\mu^-\mu^-, e^-\mu^+\mu^-, \mu^-\mu^+\mu^-)$ [9]. The analysis is based on data recorded by the *BABAR* detector at the PEP-II asymmetric-energy e^+e^- storage rings operated at the Stanford Linear Accelerator Center. The data sample consists of 339 fb^{-1} recorded at $\sqrt{s} = 10.58$ GeV, and 37 fb^{-1} recorded at $\sqrt{s} = 10.54$ GeV. With an expected cross section for tau pairs at the luminosity-weighted $\sqrt{s}$ of $\sigma_{\tau\tau} = 0.919 \pm 0.003$ nb [10], this data sample contains about 690×10^6 tau decays.

The *BABAR* detector is described in detail in Ref. [11]. Charged-particle (track) momenta are measured with a 5-layer double-sided silicon vertex tracker and a 40-layer helium-isobutane drift chamber inside a 1.5-T superconducting solenoidal magnet. The transverse momentum resolution is parameterized as $\sigma p_T / p_T = (0.13_{p_T}/[\text{GeV}/c] + 0.45)\%$. An electromagnetic calorimeter consisting of 6580 CsI(Tl) crystals is used to identify electrons and photons, a ring-imaging Cherenkov detector is used to identify charged hadrons, and the instrumented magnetic flux return (IFR), embedded with limited streamer tubes and resistive plate chambers, is used to identify muons.

A Monte Carlo (MC) simulation of lepton-flavor violating tau decays is used to optimize the parameter space for the search. Simulated tau-pair events including higher-order radiative corrections are generated using KK2F [12] with one tau decaying to three leptons with a three-body phase space distribution, while the other tau decays according to measured rates [13] simulated with TAUOLA [14]. Final-state radiative effects are simulated for all decays using PHOTOS [15]. The detector response is simulated with GEANT4 [16], and the simulated events are then reconstructed in the same manner as the data.

The signature of the decay $\tau^- \to \ell^-\ell^+\ell^-$ is a set of three charged particles, each identified as either an electron or muon, with an invariant mass and energy equal to that of the parent tau lepton. Candidate signal events in this analysis are required to have a "1–3 topology," where one tau decay yields three charged particles, while the second tau decay yields one charged particle. Events with four well-reconstructed tracks and zero net charge are selected, and the tracks are required to point toward a common region consistent with $\tau^+\tau^-$ production and decay. The polar angle of all four tracks in the laboratory frame is required to be within the calorimeter acceptance range. Pairs of oppositely charged tracks are ignored if their invariant mass, assuming electron mass hypotheses, is less than 30 MeV/c^2, as these tracks are likely to be from photon conversions in the traversed material. The event is divided into hemispheres in the e^+e^- center-of-mass (c.m.) frame using the plane perpendicular to the thrust axis, as calculated from the observed tracks and neutral energy deposits. The signal hemisphere must contain exactly three tracks while the other hemisphere must contain exactly one.

Each of the charged particles found in the signal hemisphere must be identified as either an electron or muon candidate. Electrons are identified using the ratio of calorimeter energy to track momentum (E/p), the ionization loss in the tracking system (dE/dx), and the shape of the shower in the calorimeter. Muon identification makes use of a neural net, inputs to which include the number of hits in the IFR, the number of interaction lengths traversed, and the energy deposition in the calorimeter. Muons with momentum less than 500 MeV/c do not penetrate far enough into the IFR to be identified. For the lepton momentum spectrum predicted by the signal MC calculation, the electron and muon identification requirements are found to have an average efficiency per lepton of 91% and 65%, respectively. The probability for a pion to be misidentified as an electron in three-prong tau decays is 2.7%, while the probability to be misidentified as a muon is 2.9%.

The particle identification (PID) requirements are not sufficient to suppress certain backgrounds, particularly those from light-quark pair production and higher-order radiative Bhabha and $\mu^+\mu^-$ events that can have four leptons in the final state. To reduce these backgrounds, additional selection criteria are applied to the six different decay modes. For all decay modes, the momentum of the track in the 1-prong hemisphere is required to be less than 4.8 GeV/c in the c.m. frame. For signal events, the missing momentum is given by the momentum of the neutrino(s) coming from the tau in the one-prong hemisphere. The invariant mass of that hemisphere is calculated from the total missing momentum and energy combined with the one-prong track four-momentum, assuming the most-likely mass hypothesis for that track. The mass of the

one-prong hemisphere is required to be consistent with or
smaller than the tau mass for all decay modes. For the
$e^- e^+ e^-$ and $\mu^- e^+ e^-$ decay modes, radiative Bhabha
events are suppressed by rejecting events with pairs of
oppositely-charged electron tracks in the three-prong
hemisphere with invariant mass less than 250 MeV/c^2.
For the $e^- e^+ e^-$ and $e^- \mu^+ \mu^-$ decay modes, the charged
particle in the one-prong hemisphere is required to deposit
energy in the calorimeter, and must not be identified as an
electron, while for the $\mu^- e^+ e^-$ and $\mu^- \mu^+ \mu^-$ decay
modes this track must not be identified as a muon. For
the $e^- e^+ e^-$ and $e^- \mu^+ \mu^-$ decay modes, the net transverse
momentum of the four tracks must be greater than
400 MeV/c, while for the $\mu^- e^+ e^-$ mode it must be
greater than 200 MeV/c. Events in all six decay modes
are required to have no track in the three-prong hemisphere
that is consistent with being a kaon.

To reduce backgrounds further, candidate signal events
are required to have an invariant mass and total energy in
the three-prong hemisphere consistent with a parent tau
lepton. These quantities are calculated from the observed
track momenta assuming lepton masses that correspond to
the specific decay mode. The energy difference is defined
as $\Delta E \equiv E^{\star}_{\mathrm{rec}} - E^{\star}_{\mathrm{beam}}$, where $E^{\star}_{\mathrm{rec}}$ is the total energy of the
tracks observed in the three-prong hemisphere and $E^{\star}_{\mathrm{beam}}$ is
the beam energy, with both quantities measured in the c.m.
frame. The mass difference is defined as $\Delta M \equiv M_{\mathrm{rec}} - m_{\tau}$
where M_{rec} is the reconstructed invariant mass of the three
tracks and $m_{\tau} = 1.777$ GeV/c^2 is the tau mass [13].

The signal distributions in the (ΔM, ΔE) plane (see
Fig. 1) are broadened by detector resolution and radiative
effects. In all decay modes, the radiation of photons from
the incoming $e^+ e^-$ particles and from the outgoing tau
particles leads to a tail at low values of ΔE. Radiation from
the final-state leptons, which is more likely for electrons
than for muons, produces a tail at low values of ΔM as well.
Rectangular signal regions are defined separately for each
decay mode. The signal region boundaries are chosen to
provide the smallest expected upper limits on the branch-
ing fractions in the background-only hypothesis. These
expected upper limits are estimated using only MC simu-
lations and data control samples, not candidate signal
events. For all six decay modes, the upper right corner of
the signal region in the (ΔM, ΔE) plane is fixed at (20,50),
while the lower left corner is at $(-50, -200)$ for the
$\mu^- e^+ e^-$ and $e^- \mu^+ \mu^-$ decay modes, $(-70, -200)$ for
$e^- e^+ e^-$, $(-100, -350)$ for $\mu^+ e^- e^-$, $(-50, -200)$ for
$e^+ \mu^- \mu^-$, and $(-20, -200)$ for $\mu^- \mu^+ \mu^-$. All values are
given in units of (MeV/c^2, MeV). Figure 1 shows the
observed data in the (ΔM, ΔE) plane, along with the signal
region boundaries and the expected signal distributions. To
avoid bias, a blinded analysis procedure was followed with
the number of data events in the signal region remaining
unknown until the selection criteria were finalized and all
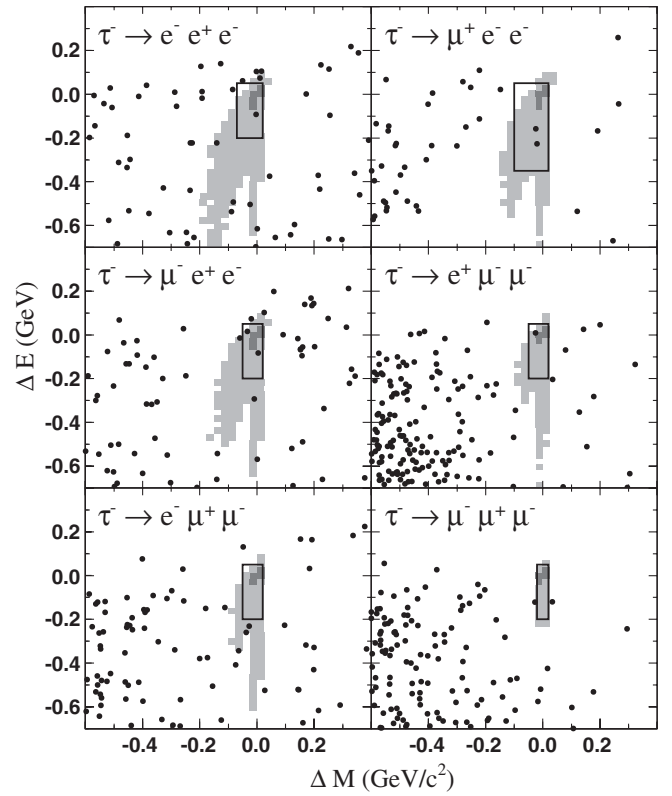cross checks were performed.

FIG. 1. Observed data shown as dots in the (ΔE, ΔM) plane
and the boundaries of the signal region for each decay mode. The
dark and light shading indicates contours containing 50% and
90% of the selected MC signal events, respectively.

There are three main classes of background remaining
after the selection criteria are applied: low multiplicity $q\bar{q}$
events (mainly continuum light-quark production); QED
events (Bhabha and $\mu^+ \mu^-$); and SM $\tau^+ \tau^-$ events. These
three background classes have distinctive distributions in
the (ΔE, ΔM) plane. The $q\bar{q}$ events tend to populate
uniformly the region $\Delta E < 0.1$ GeV/c^2 and exhibit a
broad peak unrelated to m_{τ} in ΔM, while QED back-
grounds are restricted to a narrow band at positive values
of ΔE, and $\tau^+ \tau^-$ backgrounds are restricted to negative
values of both ΔE and ΔM. A negligible two-photon
background remains.

The expected background rates for each decay mode are
determined by fitting a set of probability density func-
tions (PDFs) to the observed data in the grand side-
band (GS) region of the (ΔE, ΔM) plane. The GS region,
shown in Fig. 1, lies between -600 and 400 MeV/c^2 in
ΔM and -700 and 400 MeV in ΔE, excluding the signal
region. For the $q\bar{q}$ background, a PDF is constructed from
the product of two PDFs $P_{M'}$ and $P_{E'}$, where $P_{M'}(\Delta M')$ is a
bifurcated Gaussian and $P_{E'}(\Delta E') = (1 - x/\sqrt{1 + x^2}) \times
(1 + ax + bx^2 + cx^3)$ with $x = (\Delta E' - d)/e$. The ($\Delta M'$,
$\Delta E'$) axes have been slightly rotated from (ΔM, ΔE) to
take into account the observed correlation between ΔE and
ΔM for the distribution. The resulting PDF has a total of

eight fit parameters, including the rotation angle, all of which are determined by fits to MC $q\bar{q}$ background samples for each decay mode. For the $\tau^+\tau^-$ background PDF, the function $P_{M''}(\Delta M'')$ is the sum of two Gaussians with common mean, while the functional form of $P_{E''}(\Delta E'')$ is the same as that for the $q\bar{q}$ PDF. To properly model the wedge-shaped distribution due to the kinematic limit in tau decays, a coordinate transformation of the form $\Delta M'' = \cos\beta_1\Delta M + \sin\beta_1\Delta E$ and $\Delta E'' = \cos\beta_2\Delta E - \sin\beta_2\Delta M$ is performed. In total there are 11 free parameters describing this PDF, and all are determined by fits to the MC $\tau^+\tau^-$ samples.

For the three decay channels in which there is a significant QED background, an analytic PDF is constructed from the product of a Crystal Ball function [17] in $\Delta E'$ and a third-order polynomial in $\Delta M'$, where again the ($\Delta M'$, $\Delta E'$) axes have been rotated slightly from (ΔE, ΔM) to fit the observed distribution. The six parameters of this PDF, including the rotation angle, are obtained by fitting data control samples that are enhanced in Bhabha or $\mu^+\mu^-$ events.

With the shapes of the three background PDFs determined, an unbinned maximum likelihood fit to the data in the GS region is used to find the expected background rate in the signal region, shown in Table I. The PDF shape determinations and background fits are performed separately for each of the six decay modes.

The efficiency of the selection for signal events is estimated with a MC simulation of lepton-flavor violating tau decays. About 40% of the MC signal events pass the 1–3 topology requirement. The total efficiency for signal events to be found in the signal region is shown in Table I for each decay mode and ranges from 5.5% to 12.4%. This efficiency includes the 85% branching fraction for 1-prong tau decays.

The PID efficiencies and misidentification probabilities have been measured with control samples both for data and for MC events, as a function of particle momentum, polar angle, and azimuthal angle in the laboratory frame. The systematic uncertainties related to PID have been estimated from the statistical uncertainties of the efficiency

measurements and from their discrepancies between data and Monte Carlo calculation, and range from 2.3% for $e^-e^+e^-$ to 12.5% for $\mu^-\mu^+\mu^-$ [18]. The modeling of the tracking efficiency contributes an additional 1% uncertainty. All other sources of uncertainty in the signal efficiency are found to be small, including the statistical limitation of the MC signal samples, modeling in the generator of radiative effects, track momentum resolution, trigger performance, observables used in the selection criteria, and knowledge of the tau one-prong branching fractions. The signal efficiency has been estimated using a 3-body phase space model and no additional uncertainty is assigned for possible model dependence. Despite the effect of slow muons on the PID efficiency, the total selection efficiency is found to be uniform within 20% across 95% of the phase space for the three leptons.

Since the background levels are extracted directly from the data, systematic uncertainties on the background estimation are directly related to the background parameterization and the fit technique used. The finite data available in the GS region to determine the background rates contributes a significant uncertainty in all decay channels. Uncertainties related to the background PDFs are estimated by varying the background shape parameters within their errors and repeating the fits, and from changing the functional form of the PDFs. The total uncertainties on the background estimates are shown in Table I. Cross checks of the background estimation are performed by considering the number of events expected and observed in sideband regions immediately neighboring the signal region for each decay mode.

The numbers of events observed (N_{obs}) and the background expectations (N_{bgd}) are shown in Table I, with no significant excess found in any decay mode. Upper limits on the branching fractions are calculated according to $\mathcal{B}_{\text{UL}}^{90} = N_{\text{UL}}^{90}/(2\varepsilon\mathcal{L}\sigma_{\tau\tau})$, where N_{UL}^{90} is the 90% C.L. upper limit for the number of signal events when N_{obs} events are observed with N_{bgd} background events expected. The values ε, $\mathcal{L}$, and $\sigma_{\tau\tau}$ are the selection efficiency, luminosity, and $\tau^+\tau^-$ cross section, respectively. The uncertainty on the product $\mathcal{L}\sigma_{\tau\tau}$ is 1.0%. The branching fraction upper limits are calculated including all uncertainties using the technique of Cousins and Highland [19] following the implementation of Barlow [20]. The sensitivity or expected upper limit $\text{UL}_{90}^{\text{exp}}$, defined as the mean upper limit expected in the background-only hypothesis, is included in Table I. The 90% C.L. upper limits on the $\tau^- \to \ell^-\ell^+\ell^-$ branching fractions are in the range $(4\text{–}8) \times 10^{-8}$. These limits represent up to an order of magnitude improvement over the previous experimental bounds [21,22].

TABLE I. Efficiency estimates, number of expected background events (N_{bgd}), expected branching fraction upper limits at 90% C.L. ($\text{UL}_{90}^{\text{exp}}$), number of observed events (N_{obs}), and observed branching fraction upper limits at 90% C.L. ($\text{UL}_{90}^{\text{obs}}$) for each decay mode. All upper limits are in units of 10^{-8}.

Mode	Eff. [%]	N_{bgd}	$\text{UL}_{90}^{\text{exp}}$	N_{obs}	$\text{UL}_{90}^{\text{obs}}$
$e^-e^+e^-$	8.9 ± 0.2	1.33 ± 0.25	4.9	1	4.3
$\mu^-e^+e^-$	8.3 ± 0.6	0.89 ± 0.27	5.0	2	8.0
$\mu^+e^-e^-$	12.4 ± 0.8	0.30 ± 0.55	2.7	2	5.8
$e^+\mu^-\mu^-$	8.8 ± 0.8	0.54 ± 0.21	4.6	1	5.6
$e^-\mu^+\mu^-$	6.2 ± 0.5	0.81 ± 0.31	6.6	0	3.7
$\mu^-\mu^+\mu^-$	5.5 ± 0.7	0.33 ± 0.19	6.7	0	5.3

---

*Deceased.

†Present address: Tel Aviv University, Tel Aviv, 69978, Israel.

‡Also with Università di Perugia, Dipartimento di Fisica, Perugia, Italy.

§Also with Università della Basilicata, Potenza, Italy.

‖Also with Universitat de Barcelona, Facultat de Fisica, Departament ECM, E-08028 Barcelona, Spain.

[1] M. L. Brooks *et al.* (MEGA/LAMPF Collaboration), Phys. Rev. Lett. **83**, 1521 (1999).

[2] U. Bellgardt *et al.* (SINDRUM Collaboration), Nucl. Phys. B **299**, 1 (1988).

[3] M. H. Ahn *et al.* (K2K Collaboration), Phys. Rev. Lett. **90**, 041801 (2003); K. Eguchi *et al.* (KamLAND Collaboration), Phys. Rev. Lett. **90**, 021802 (2003); Q. R. Ahmad *et al.* (SNO Collaboration), Phys. Rev. Lett. **89**, 011301 (2002); Y. Fukuda *et al.* (Super-Kamiokande Collaboration), Phys. Rev. Lett. **81**, 1562 (1998).

[4] X. Y. Pham, Eur. Phys. J. C **8**, 513 (1999).

[5] K. Hayasaka *et al.* (Belle Collaboration), arXiv:0705.0650.

[6] P. Paradisi, J. High Energy Phys. 10 (2005) 006.

[7] K. S. Babu and C. Kolda, Phys. Rev. Lett. **89**, 241802 (2002).

[8] A. Brignole and A. Rossi, Phys. Lett. B **566**, 217 (2003).

[9] Throughout this Letter, charge conjugate decay modes also are implied.

[10] S. Banerjee, B. Pietrzyk, J. M. Roney, and Z. Wäs, arXiv:0706.3235.

[11] B. Aubert *et al.* (*BABAR* Collaboration), Nucl. Instrum. Methods Phys. Res., Sect. A **479**, 1 (2002).

[12] B. F. Ward, S. Jadach, and Z. Wäs, Nucl. Phys. B, Proc. Suppl. **116**, 73 (2003).

[13] Y.-M. Yao *et al.* (Particle Data Group), J. Phys. G **33**, 1 (2006).

[14] S. Jadach, Z. Wäs, R. Decker, and J. H. Kühn, Comput. Phys. Commun. **76**, 361 (1993).

[15] E. Barberio and Z. Wäs, Comput. Phys. Commun. **79**, 291 (1994).

[16] S. Agostinelli *et al.* (GEANT4 Collaboration), Nucl. Instrum. Methods Phys. Res., Sect. A **506**, 250 (2003).

[17] M. J. Oreglia, Ph.D. thesis, SLAC-236, 1980, Appendix D; J. E. Gaiser, Ph.D. thesis, SLAC-255, 1982, Appendix F; T. Skwarnicki, Ph.D. thesis, DESY F31-86-02, 1986, Appendix E.

[18] All uncertainties quoted in the text are relative.

[19] R. D. Cousins and V. L. Highland, Nucl. Instrum. Methods Phys. Res., Sect. A **320**, 331 (1992).

[20] R. Barlow, Comput. Phys. Commun. **149**, 97 (2002).

[21] B. Aubert *et al.* (*BABAR* Collaboration), Phys. Rev. Lett. **92**, 121801 (2004).

[22] Y. Yusa *et al.* (Belle Collaboration), Phys. Lett. B **589**, 103 (2004).